Light-Independent Feature Detection using Intensity Data of Laser Range Finder

Kentaro Kimura*, Genya Ishigami*

*Graduate School of Science and Engineering, Keio University
e-mail: wakametchi@z3.keio.jp, ishigami@mech.keio.ac.jp

Abstract

This paper describes a preprocessing method for a robust feature detection under extreme lighting environment. The feature detection is widely used on the computer vision, nevertheless one of its technical problem is that it is not robust to lighting environment. This research focuses on an intensity image provided from Laser Range Finder. The intensity image is equivalent to a magnitude of the reflected light emitted from the LRF. The proposed method exploits the camera image and the intensity image conplementarily: first, the camera image is preprocessed such of the image that each pixel is labeled based on its lighting condition. Subsequently, the intensity image is combined with the camera image and the number of features from both images are regulated in accordance with their feature quantity. The proposed method is validated in both indoor/outdoor field experiment.

1 Introduction

Mobile robots or rovers play a significant role in exploring extreme environment such as planetary surfaces. For example, Mars Science laboratory, Curiosity, has succeeded to make a soft landing on Mars surface in 2012. Until now on, the Curiosity rover has been analyzing possibility of lives. Like this, Mobile Robots investigating these extreme environment present a lot of meanings for human beings, and it can say that they have significant social expectation from people all over the world.

One promising way to move these robots is a teleoperation controlling, but the communication delay between the Earth and target body should be taken into account. Therefore, an autonomous mobility system is required to compensate the communication delay.

One of the most commonly used sensors in autonomous mobile robot is camera. Visual information provided from the camera enables the rover to execute a visual odometry[1] for its localization, or a stereo vision can generate a three dimentional terrain map around the rover[2]. A key issue in such vision-based task is to detect good feature points to be tracked in a scene. However, the feature detection has a technical problem, feature can't be well detected on an environment where a light condition is too dark or too bright.

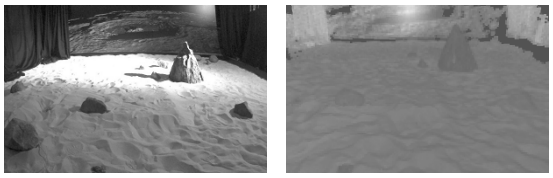

(a): Camera Image (b): Intensity Image

Figure 1. Comparison of Images

In this work, an intensity image proveded by a laser range finder (LRF) is exploited. The LRF is a distance sensor that can determine a distance from a laser emitter to an object based on the time of flight principle. In addition, LRF can also provide an image called intensity image, that consists of a set of reflection intensity from all object in its field of view. As shown in Fig. 1a and Fig. 1b, the intensity image data can be provided without effect of ambient light. This is because the camera image passively captures a reflection of ambient light, while the intensity image is given from an infrared light radiated out from the LRF. This paper uses this light-independent intensity image to conpenstate a drawback for classical method, that was caused by severe lighting environment.

This paper proposes a light-independent feature detecting method by using an intensity image provided from the LRF and a camera image complementary. By applying proposed method to the data taken in indoor environment and outdoor environment, the usefulness of the method is confirmed. The rest of this paper is organized as follows: section 2 introduces the proposed method for the lighting-independent feature detection, and explains image processing algorithm used in the proposed method. The experimental validation of the method is summarized in section 3 and 4. And conclusion in section 5.

2 Proposal of Feature Detection Method using Intensity Image

This research proposes steps below to match images between before robot's movement and after robot's movement.

1. By using pixel value of camera image, binalize image by region of extreme and fine lighting condition.

2. Process Dilation to region of fine lighting condition. Put region of fine lighting condition as "region T", and extreme one as "region F".

3. Use T and F for mask image, and detect feature by using Feature from Accelerated Segment Test (FAST) feature detector[3].

4. Extract feature values by using Binary Robust Invariant Scalable Keypoints (BRISK) feature extractor[4] for each feature points detected in previous step.

5. According to BRISK feature value, find out pairs of feature points matches between images of before movement and after movement, according to BRISK feature values. It should be done for each "region T" of camera image, "region F" of camera image, "region T" of intensity image, and "region F" of intensity image. Put point cloud matched here as ${}^{\alpha}\mathbf{K}_{matched} = [{}^{\alpha}\mathbf{k}_1, {}^{\alpha}\mathbf{k}_2, \cdots, {}^{\alpha}\mathbf{k}_m]^{\mathrm{T}}$. However, pretend that $\mathbf{k}$ as a coordinates of feature points and m_α as number of pairs matched in this step.

6. Add up pairs of matches found in region T and region F, and classify them into inliers and outliers. Put point cloud matched here as ${}^{\alpha}\mathbf{K}_{inlier} = [{}^{\alpha}\mathbf{p}_1, {}^{\alpha}\mathbf{p}_2, \cdots, {}^{\alpha}\mathbf{p}_c]^{\mathrm{T}}$. However, pretend that $\mathbf{p}$ as a coordinates of inliers and c_α as number of inliers found in this step. Subsequently, import index shown in Eq(1) as confidence rate for correct matches.

$$ {}^{\alpha}I_m = c/m \tag{1} $$

   High value of ${}^{\alpha}I_m$ can be said that feature detection was done in high precision.

By classifying camera image as region T and region F, it is possible to detect feature points of intensity image preferentially on region F. 20~30 inliers are typically regarded to be enough for estimating correct matches. In abovementioned steps, α is defined as $\alpha \equiv gT$ for region T of camera image, $\alpha \equiv gF$ for region F of camera image, $\alpha \equiv iT$ for region T of intensity image, and $\alpha \equiv iF$ for region F of intensity image.

(a): Before Binarize

(b): After Binalize

Figure 2. Example of Binarization

Figure 3. Dilation of Image

2.1 Binarize Image

In proposed method, camera image is signified in two regions, one is difficult for feature detection, and other is not. Example of difficult region for feature detection is dark region because ambient light has not reached, and region that clipped white because of too much ambient light. Therefore, regard pixel that has too much value and few value as extreme lighting condition, and classifying extreme lighting condition region and fine lighting condition region according to Eq(2).

$$ I_{x,y} = \begin{cases} 0, & (I_{x,y} < 50, I_{x,y} > 200) \\ 255, & (otherwise) \end{cases} \tag{2} $$

However, $I_{x,y}$ regards as pixel value of image, pixel value of 255 as region T, pixel value of 0 as region F, Fig. 2a and Fig. 2b shows a comparison of image before binarize and after binarize.

2.2 Dilating Image

In previous step, image was binarized on region T and region F. However, borderline between region T and region F, which means shadow, can be a good candidate for feature points. Therefore, dilating region T is needed to detect shadow as feature points. Image dilation is typically applied on binarized image, and it is to replace pixel as white if there is any white pixel surrounding. Showing dilated image on Fig. 3 which original image is Fig. 2b.

2.3 FAST Feature Detector

Feature detection means detecting remarkable pixel(keypoint) in a image. FAST Feature detctor used in this paper is first introduced by Edward Rosten and others in 2006. FAST feature detector is used in many researches since it realizes very fast detection. FAST corner detection follows steps below.

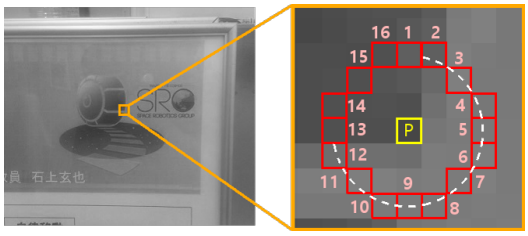

Figure 4. Detection Corner by Fast Corner Detection

1. Grayscale the image.
2. Choose one pixel **p** on image and put pixel value as I_p.
3. Set threshold T.
4. Focus on 16 pixels surrounding **p** as shown in Fig. 4 and sort out 16 pixel as brighter, similar, and darker.

$$S_{p\to x} = \begin{cases} \text{brighter}, & (I_p + T \le I_{p\to x}) \\ \text{similar}, & (I_p - T < I_{p\to x} < I_p + T) \\ \text{darker}, & (I_{p\to x} \le I_p - T) \end{cases} \tag{3}$$

However, $x \in 1, \ldots, 16$ is position of pixel, $I_{p\to x}$ is pixel value, and $S_{p\to x}$ is pixel value classified in darker, brighter, and similar.

5. If $S_{p\to x}$ becomes darker or brighter 9 times continuously, Regard **p** as corner.

In addiction to abovementioned steps, Fast corner detector uses decision tree, which applied machine learning according to the algorithm of ID3[5]. It is possible to judge weather **p** is corner or not by focusing on 2.16 pixels for each **p** by using decision tree.

2.4 BRISK Feature extractor

To match feature points, it is necessary to extract feature values for each feature point. BRISK feature extractor used in this paper is first introduced by Leutenegger and others in 2008. BRISK feature extractor uses 60 pixel values posted systematically on 4 concentric circle as shown in Fig. 5. Make pairs from 60 pixels, and express magnitude correlation as binary code. BRISK feature extractor follows steps below.

1. Apply Gausian smoothing with standard devision proportional to the distance between the points on the respective circle to avoid aliasing.
2. Regard point pairs, which has distance over δ_{max} as L, and regard point pairs, which has distance lower than δ_{min} as S. L will be used to determine overall characteristics pattern direction, and S will be feature value.

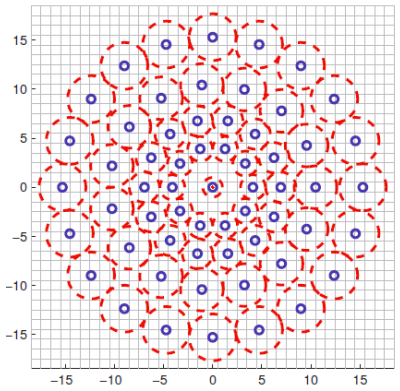

Figure 5. Patch for BRISK

3. Estimate the overall characteristics pattern direction **g** of feature point using point pairs in L. However, coordination of pairs of points regards as $\mathbf{p}_i$, $\mathbf{p}_j$ and combination of pairs are settled in advance.
4. Rotate $\mathbf{p}_i$, $\mathbf{p}_j$ according to **g**. Regard pixel after rotated as $\mathbf{p}_i^\beta$,$\mathbf{p}_j^\beta$.
5. By following eq(4), correspond b.

$$b = \begin{cases} 1, & I(\mathbf{p}_i^\beta > \mathbf{p}_j^\beta) \\ 0, & \text{otherwise} \end{cases} \tag{4}$$

Remind that pairs are from S. δ_{min} is settled to be S has 512 pairs, so binary code will be 512 bit.

3 Experiment under controlled ambient light

3.1 Experimental Outlines

To demonstrate that proposed method is effective, experiment was done on indoor sand field equipped in JAXA Sagamihara Campus shown in Fig. 6. This field has 7 lighting equipments, which can turn off/on so that lighting environment can be changed. In this work, following three cases of lighting environment mentioned below were done.

1. Turn all lighting equipments off: experimental environment is dark.
2. Turn all lighting equipments on: experimental environment is well-lighted.
3. Turn only one lighting equipments on: shadow appears on experimental environment.

Figure 6. Experimental Environment

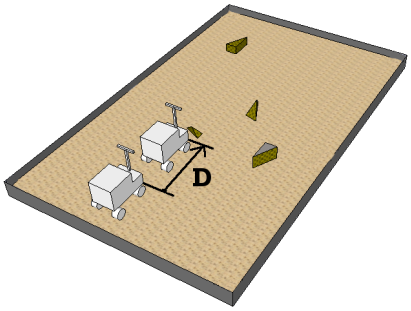

Figure 7. Schematic Illustration of Robot Displacement

Displacement of measurement position is D, regard initial displacement as 0 cm, and move measurement position straightfoward by 5 cm as shown in Fig. 7. Confidence rate of each classical method, which is only using camera image, and proposed method, which is using both camera image and intensity image is to be investigated. Confidence rate of classical method is ${}^{g}I_m$, proposed method is ${}^{p}I_m$. To examine the data, confidence rate of method using only intensity image ${}^{i}I_m$ was investigated also. As shown in Fig. 6 bottom of this sand field is partitioned by curtain although feature point of the sand field surface is needed. So mask for above 1/3 of image is applied.

3.2 Experimental Result and Examination(Case 1)

Fig. 8a and Fig. 8b shows each camera image and intensity image of environment under Case 1. Region T and regin F turned out to be as shown in Fig. 9a and Fig. 9b. Fig. 10 shows the graph of confidence rate toward moving distance D, and Fig. 11a and Fig. 11b shows example of inliers for each classical method and proposed method on $D = 5$ cm. X-axis of graph stands for moving distance and

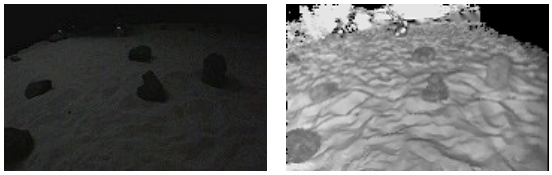

(a): Camera Image (b): Intensity Image

Figure 8. Image Data of Case 1(D=0)

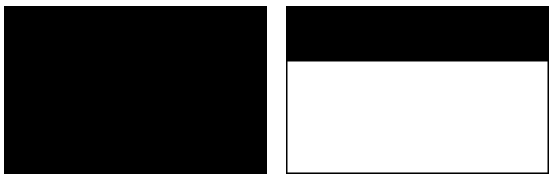

(a): Mask Image T (b): Mask Image F

Figure 9. Mask Image of Case 1(D=0)

Y-axis stands for confidence rate. Camera, Intensity, and Proposed regards each confidence rate of classical method ${}^{g}I_m$, confidence rate of only using intensity image ${}^{i}I_m$, and confidence rate of proposed method ${}^{p}I_m$.

As shown in Fig. 10, confidence rate of proposed method ${}^{p}I_m$ has significantly overcomed confidence rate of classical method used so far ${}^{g}I_m$ in all moving distance. Considering from this, intensity image has detected feature points of region in extreme lighting environment instead of camera image. Moreover, camera image had difficulty detecting feature points of texture of sand, while intensity image can. So proposed method could detect surface of sandbox as inliers.

3.3 Experimental Result and Examination(Case 2)

Fig. 12a and Fig. 12b shows each camera image and intensity image of environment under Case 2. Region T and region F turned out to be as shown in Fig. 13a and

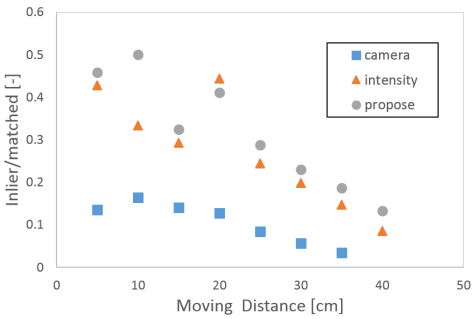

Figure 10. Experimental Result(Case 1)

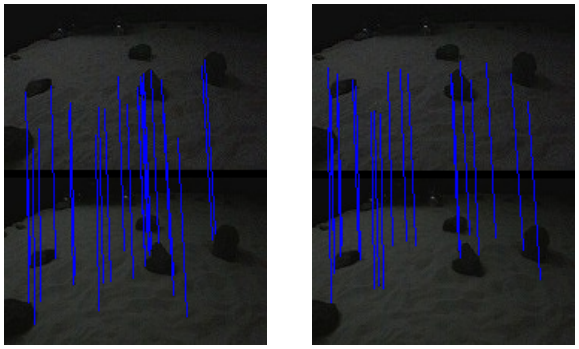

(a): Classical Method (b): Proposed Method

Figure 11. Matching Result in Case 1

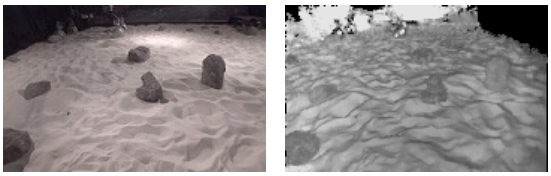

(a): Camera Image (b): Intensity Image

Figure 12. Image Data of Case 2(D=0)

Fig. 13b. Fig. 14 shows the graph of confidence rate toward moving distance D, and Fig. 15a and Fig. 15b shows example of inliers for each classical method and proposed method on D = 5 cm.

As shown in Fig. 14, confidence rate of proposed method ${}^{p}I_m$ has overcomed confidence rate of classical method ${}^{g}I_m$ except D = 5 cm. Most inliers for camera image were observed on border between sand and rock, but surface of sand field were sharper for intensity image, so proposed method observed more inliers on surface than classical method.

3.4 Experimental Result and Examination(Case 3)

Fig. 16a and Fig. 16b shows each camera image and intensity image of environment under Case 3. Region T and region F turned out to be as shown in Fig. 17a and Fig. 17b. Fig. 18 shows the graph of confidence rate

(a): Mask Image T (b): Mask Image F

Figure 13. Mask Image of Case 2(D=0)

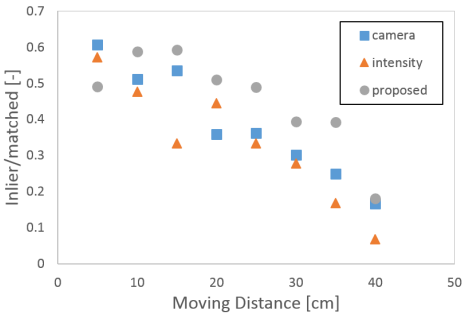

Figure 14. Experimental Result(Case 2)

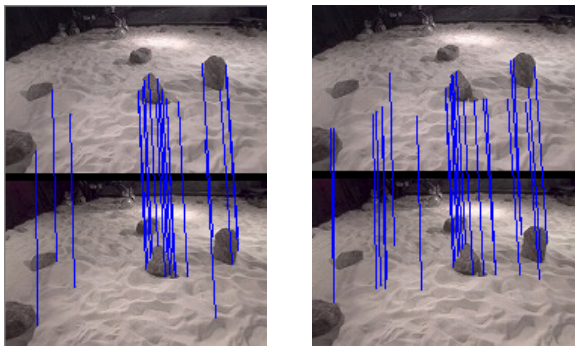

(a): Classical Method (b): Proposed Method

Figure 15. Matching Result in Case 2

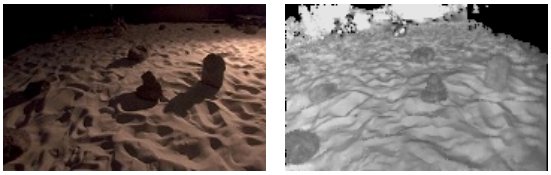

(a): Camera Image (b): Intensity Image

Figure 16. Image Data of Case 3(D=0)

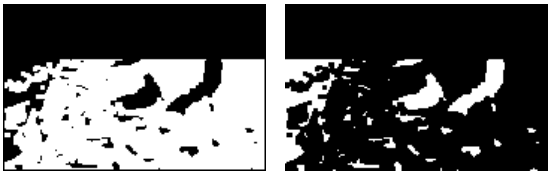

(a): Mask Image T (b): Mask Image F

Figure 17. Mask Image of Case 3(D=0)

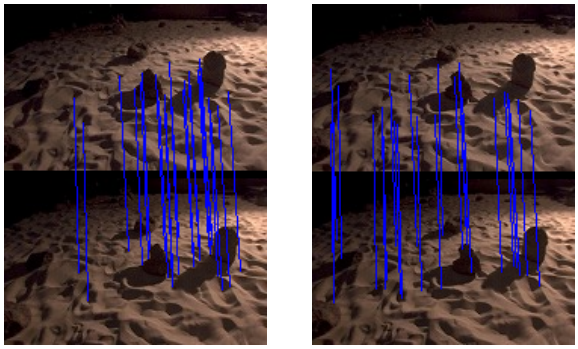

(a): Classical Method (b): Proposed Method

Figure 19. Matching Result in Case 3

toward moving distance D, and Fig. 19a and Fig. 19b shows example of inliers for each classical method and proposed method on D = 5 cm.

As shown in Fig. 18, confidence rate of proposed method ${}^{p}I_m$ has overcomed confidence rate of classical method ${}^{g}I_m$ in all moving distance. Moreover, comparing Fig. 19a and Fig. 19b, Fig. 19b is observing inliers inside the shadow and left side of the image, which can be classify as extreme lighting environment. And also, borderline of shadow is taken as inliers, too. Considering from this, proposed method has succeeded to achieve goal that taking both borderline of shadow and region with extreme lighting environment.

3.5 Considering Overall

Result of those three cases of experiment shows that proposed method is effective, especially for Case 1. Also, case 3 shows that proposed method is also effective, even

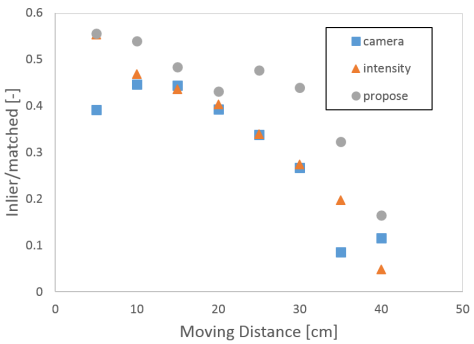

Figure 18. Experimental Result(Case 3)

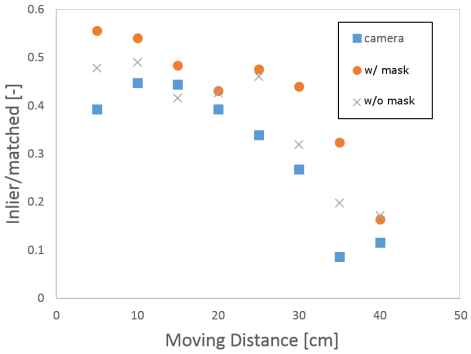

Figure 20. Experimental Result(Case 3)

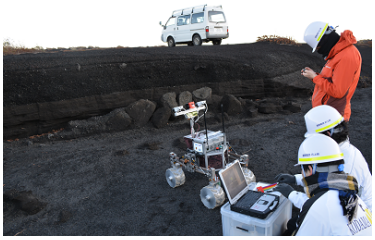

Figure 21. Experimental Environment

though case 3 differs from others: it has extreme lighting environment region and fine lighting environment region mixed, so that feature points are taken from both region T, and region F. To prove that the process, classifying image into region T and region F, had some sence, confidence rate when "not" using mask image. Confidence rate of it regards as ${}^{'p}I_m$. Fig. 20 shows each confidence rate towards moving distance. Each ${}^{g}I_m$, ${}^{p}I_m$, ${}^{'p}I_m$ regards as camera, w/ mask, and w/o mask.

4 Experiment on Outdoor Environment

4.1 Experiment Outlines

Experimental environment was conducted on desert field in Izu-Ohshima shown in Fig. 21. Human beings has did almost nothing to this field, and this field is covered with lava rocks and volcanic ash.

As same as experiment in previous section, Displacement of measurement position is D, regard initial replacement as 0 cm, and move measurement position straightfoward by 5 cm. Confidence rate of classical method, which is only using camera image, and confidence rate of proposed method, which is using both camera image and intensity image complementary is to be investigated. Confidence rate of classical method is ${}^{g}I_m$, and proposal method is ${}^{p}I_m$. To examine the data, confidence rate of method using only intensity image ${}^{i}I_m$ was investigated also.

4.2 Experimental Result and Examination

Fig. 22 and Fig. 23 shows each camera image and intensity image of outdoor environment. Region T and region F turned out to be as shown in Fig. 24a and Fig. 24b. Fig. 25 shows the graph of confidence rate toward moving distance D, and Fig. 26a and Fig. 26b shows example of inliers for each classical method and proposed method on $D = 5$ cm.

As shown in Fig. 25, proposed method was effective in all moving distance. This situation is close to Case 2 in previous section, but difference is that confidence rate of using camera image ${}^{g}I_m$ has overcomed confidence rate

Figure 22. Camera Image(D=0)

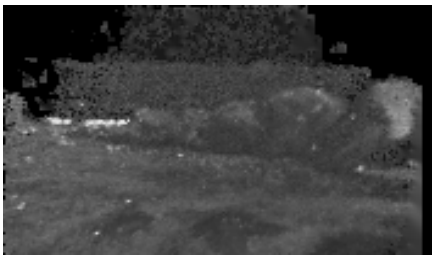

Figure 23. Intensity Image(D=0)

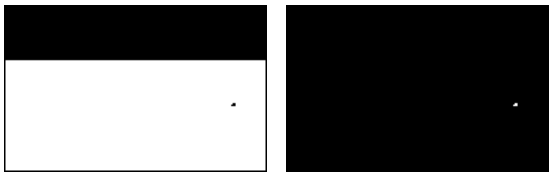

(a): Mask Image T (b): Mask Image F

Figure 24. Mask Image

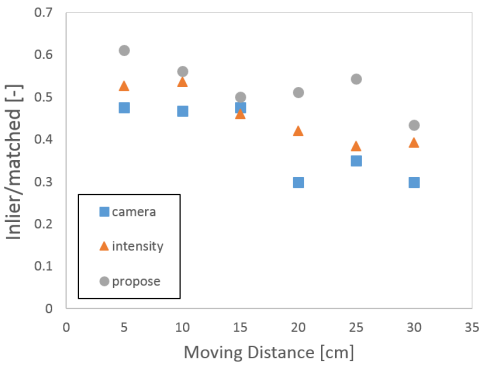

Figure 25. Experimental Result

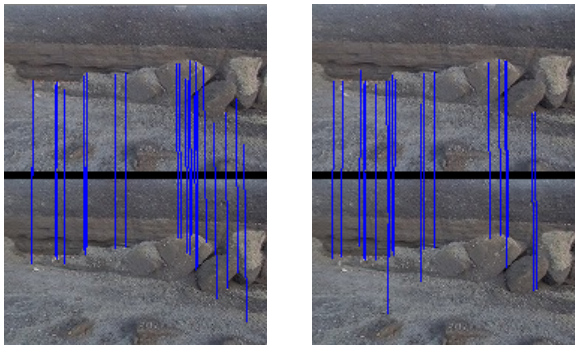

(a): Classical Method (b): Proposed Method

Figure 26. Matching Result

of using intensity image ${}^{i}I_{m}$. Reason for this can be considered that intensity image has very high pixel value in local. This high pixel value appeared because of flora on the field, which has different reflection image compared to surface of ground.

Moreover, pixel of intensity image that is value of 0 observed more in this environment than in inside environment. Pixel value of 0 for intensity image means that data was not taken well, because infrared light radiated out from LRF couldn't reflect back for the reason that target object absorbed or disperse radiated light. Considering from this, there is technical problem that using only intensity image for feature detection likewise as camera image. It means that usability of proposed method is confirmed.

5 Conclusion

This paper, has proposed a method that complementary exploits a camera image and an intensity image provided from LRF. complementary was proposed. A classical feature detection uses only camera image, depended on ambient light and is severely influenced by lighting environment. But using the intensity image, light-independent robust feature detection was achieved. The usefulness of the proposed method has been proven in three different lighting cases of indoor environment and in the field experiment in Izu-Ohshima.

This research still includes the following open issues to be solved. The current, method proposed in this paper compensates a low quality region of a camera image by the use of an intensity image are compensated one another is necessary for more accurate feature detection. Such duplex process will be useful for an object that absorbs/diffuses infrared light from the LRF.

References

[1] M. Maimone, Y. Cheng, and L. Matthies, "Two years of visual odometry on the Mars Exploration Rovers," J. of Field Robotics, Special Issue on Space Robotics, 24(3):169–186, March 2007.

[2] L. Matthies, "Stereo Vision for Planetary Rovers: Stochastic Modeling to Near Real-Time Implementation," Int. J. of Computer Vision, Vol. 8, No. 1, ,pp. 71–91, 1992.

[3] E.Rosten and T.Drummond, "Machine learning for high-speed corner detection," European Conference on computer Vision, pp430–443, 2006.

[4] S. Leutenegger, M.chli and R.Siegwart, "Brisk: Binary robust invariant scalable keypoints", Proc. of the IEEE International Conference on Computer Vision, ICCV, 2011.

[5] J.R.Quinlan, "Induction of decision trees," Machine Learning 1, pp. 81–106, 1986.